

Mechanistic Requirements for the Efficient Enzyme-Catalyzed Hydrolysis of Thiosialosides[†]

Arun A. Narine, Jacqueline N. Watson, and Andrew J. Bennet*

Department of Chemistry, Simon Fraser University, 8888 University Drive, Burnaby, British Columbia V5A 1S6, Canada

Received April 18, 2006; Revised Manuscript Received June 10, 2006

ABSTRACT: The sialidase from *Micromonospora viridifaciens* has been found to catalyze the hydrolysis of aryl 2-thio- α -D-sialosides with remarkable efficiency: the first- and second-order rate constants, k_{cat} and $k_{\text{cat}}/K_{\text{m}}$, for the enzyme-catalyzed hydrolysis of PNP-S-NeuAc are $196 \pm 5 \text{ s}^{-1}$ and $(6.7 \pm 0.7) \times 10^5 \text{ M}^{-1} \text{ s}^{-1}$, respectively. A reagent panel of eight aryl 2-thio- α -D-sialosides was synthesized and used to probe the mechanism for the *M. viridifaciens* sialidase-catalyzed hydrolysis reaction. In the case of the wild-type enzyme, the derived Brønsted parameters (β_{lg}) on k_{cat} and $k_{\text{cat}}/K_{\text{m}}$ are -0.83 ± 0.11 and -1.27 ± 0.17 for substrates with thiophenoxide leaving groups of pK_{a} values ≥ 4.5 . For the general-acid mutant, D92G, the derived β_{lg} value on k_{cat} for the same set of leaving groups is -0.82 ± 0.12 . When the conjugate acid of the departing thiophenol was ≤ 4.5 , the derived Brønsted slopes for both the wild-type and the D92G mutant sialidase were close to zero. In contrast, the nucleophilic mutant, Y370G, did not display a similar break in the Brønsted plots, and the corresponding values for β_{lg} , for the three most reactive aryl 2-thiosialosides, on k_{cat} and $k_{\text{cat}}/K_{\text{m}}$ are -0.76 ± 0.28 and -0.84 ± 0.04 , respectively. Thus, for the Y370G enzyme glycosidic C–S bond cleavage is rate-determining for both k_{cat} and $k_{\text{cat}}/K_{\text{m}}$, whereas, for both the wild-type and D92G mutant enzymes, the presented data are consistent with a change in rate-determining step from glycosidic C–S bond cleavage for substrates in which the pK_{a} of the conjugate acid of the leaving group is ≥ 4.5 , to either deglycosylation (k_{cat}) or a conformational change that occurs prior to C–S bond cleavage ($k_{\text{cat}}/K_{\text{m}}$) for the most activated leaving groups. Thus, the enzyme-catalyzed hydrolysis of 2-thiosialosides is strongly catalyzed by the nucleophilic tyrosine residue, yet the C–S bond cleavage does not require the conserved aspartic acid residue (D92) to act as a general-acid catalyst.

The family of enzymes that cleave terminal sialic acid residues from glycoconjugates is called exosialidases (*N*-acetylneuraminosyl glycohydrolases, neuraminidases, EC 3.2.1.18) (1). Of the approximately 100 sequence-based glycosidase families, exosialidases have been classified into families 33, 34, and 83 (2–4). Within the exosialidase superfamily, sequence homology and X-ray crystal structure data have revealed that seven amino acid residues are strictly conserved in the enzyme active site (5). As a consequence of these homologies, it is not surprising that all known exosialidases operate via similar double displacement reactions, a mechanism that was first proposed by Koshland, over 50 years ago, for retaining acetal-hydrolyzing glycosidases (6–10).

Recently, two separate experimental approaches have implicated the conserved tyrosine residue, rather than either the proximal glutamate or aspartate residues, as the catalytic nucleophile (11, 12). Specifically, Withers and co-workers used a 3-fluorosialosyl fluoride to label the critical tyrosine residue covalently in both a *Trypanosoma rangeli* sialidase (13, 14) and a *Trypanosoma cruzi* trans-sialidase active site mutant (12) for further mass spectral and X-ray crystallographic characterization. Bennet and co-workers, using site-

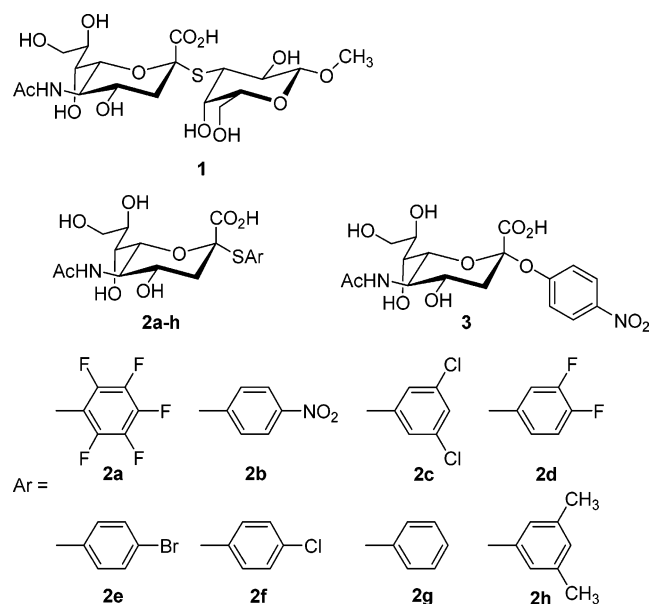
directed mutagenesis, replaced the active site tyrosine residue in the *Micromonospora viridifaciens* sialidase with several amino acids, such as aspartate, a modification that changed the hydrolytic mechanism from one involving retention of anomeric configuration to one where the reaction proceeded with a single inversion at the anomeric center (11, 15, 16). The conserved active site aspartate residue has been postulated to be the general-acid catalyst (17), and in the case of *M. viridifaciens* sialidase, this residue has been shown to make a significant energetic contribution (i.e., 19 kJ/mol) to the hydrolysis of natural substrates (18). The third catalytic residue, a conserved glutamic acid, is presumed to act as a general-base catalyst facilitating attack of the tyrosine nucleophile (11, 16).

The 65 kDa sialidase from the soil bacterium *M. viridifaciens* has been cloned and recombinantly expressed in *Escherichia coli* (11). Of note, this sialidase is rather promiscuous, in that it has the ability to hydrolyze, at similar rates, both 2,3- and 2,6-sialyllactose (11) as well as 2,8-linked polysialic acid (19). In addition, the *M. viridifaciens* sialidase is able to process efficiently a broad range of substrate types displaying high catalytic proficiencies (CP)¹ [$\text{CP} = (k_{\text{cat}}/K_{\text{m}})/k_{\text{uncat}}$] (20). For instance, in the case of pyridinium α -D-sialosides the measured CP value for the *M. viridifaciens* sialidase is 2–3 orders of magnitude greater than those determined for several bacterial and viral sialidases

[†] This work was supported by the Natural Sciences and Engineering Research Council of Canada.

* To whom correspondence should be addressed. E-mail: bennet@sfu.ca. Tel: (604) 291-4884. Fax: (604) 291-5424.

(21). Interestingly, this enzyme displays similarly high catalytic efficiencies with both activated and natural substrates ($k_{\text{cat}}/K_m \sim 10^5\text{--}10^7 \text{ M}^{-1} \text{ s}^{-1}$) (11). To delineate the structural features of the *M. viridifaciens* sialidase responsible for its unique activity, several X-ray crystallographic studies have been performed (15, 18, 22, 23). However, to date, it has not been possible to observe by X-ray crystallography either a substrate or a substrate analogue bound in the active site of the *M. viridifaciens* sialidase. Given that *exo*-thioglycosides, compounds where the glycosidic oxygen has been substituted with a sulfur atom, have been used as nonhydrolyzable substrate analogues in several X-ray crystal structures of thioglycoside–glycosidase complexes (24, 25), it was decided to evaluate the potential use of a simple aryl 2-thio- α -D-sialoside for X-ray crystallographic analysis of the *M. viridifaciens* sialidase. In addition, it has been reported that the *Vibrio cholerae* sialidase is incapable of hydrolyzing α -Neup5Ac-(2 \rightarrow 3)-3-*S*- β -D-galpOMe (**1**) (26). However, an initial screen showed that the *M. viridifaciens* sialidase displayed a significant activity toward aryl 2-thio- α -D-sialosides.



Consequently, the present paper details a kinetic study performed using a panel of substituted aryl 2-thio- α -D-sialosides (**2a–h**) with the *M. viridifaciens* sialidase. The kinetic data are compared to those obtained for a standard and commercially available sialidase substrate, PNP-*O*-NeuAc (**3**). In addition to the wild-type enzyme, catalytic mutants Y370G and D92G, lacking the nucleophilic and general-acid residues, respectively, were characterized in order to determine the mechanistic requirements for efficient hydrolysis of thiosialosides.

MATERIALS AND METHODS

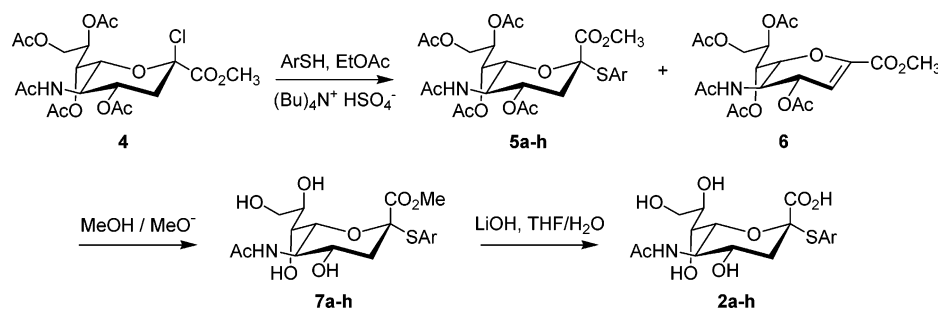
Materials. PNP-*O*-NeuAc was synthesized according to literature methods (27, 28). All thiophenols were purchased

from Sigma-Aldrich and used without further purification. Full experimental details for the synthesis of **2b** are given below while those for **2a** and **2c–h** are given in the Supporting Information section. MU-NeuAc and NeuAc were purchased from Rose Scientific and used without further purification. Milli-Q water ($18.2 \text{ M}\Omega \text{ cm}^{-1}$) was used for kinetic and product study experiments. All other salts used in the hydrolysis runs were of analytical grade and were not purified further. All pH values were measured using a Radiometer pHM82 standard pH meter and a standard combination glass electrode standardized with Fisher certified buffers (pH = 4.0, 7.0, and 10.0). NMR spectra were acquired on Bruker AMX-400, Varian Unity-500, or Bruker AMX 600 spectrometers. Chemical shifts are reported in parts per million downfield from signals for TMS. The residual signals from deuterated chloroform and external TMS salt (D_2O) were used for ^1H NMR spectral references; for ^{13}C NMR spectra, natural abundance signals from CDCl_3 and external TMS salt (D_2O) were used as references. Coupling constants (J) are given in hertz. Melting points were determined on a Gallenkamp melting point apparatus and are not corrected, and optical rotations were measured on a Perkin-Elmer 341 polarimeter.

4-Nitrophenyl 5-Acetamido-3,5-dideoxy-2-thio-D-glycero- α -D-galacto-2-nonulopyranosidonic Acid (2b**).** To a stirred solution of sialosyl chloride **4** (29) (1.00 g, 1.96 mmol) and tetra-*n*-butylammonium bisulfate (0.68 g, 1.9 mmol, 97% purity) in ethyl acetate (20 mL) at room temperature was added 4-nitrothiophenol (0.49 g, 2.5 mmol, 80% purity) in aqueous sodium carbonate (20 mL, 1 M). After 1.5 h, the bright orange/red reaction mixture was diluted with ethyl acetate (100 mL) and washed with a saturated aqueous solution of sodium bicarbonate ($3 \times 50 \text{ mL}$) and brine (50 mL). The organic layer was dried over anhydrous magnesium sulfate, filtered, and concentrated under reduced pressure to afford a bright red foam. Purification by silica gel chromatography using ethyl acetate–hexanes (1:1) and then ethyl acetate as eluent afforded an inseparable mixture (875 mg, 86:14) of the peracetylated thiosialoside **5b** (30, 31) and the glycal **6**: ^1H NMR (CDCl_3) δ 1.88 (s, 3 H, Ac), 2.03 (s, 3 H, Ac), 2.04 (s, 3 H, Ac), 2.06 (s, 3 H, Ac), 2.09 (m, 1 H, H-3ax), 2.16 (s, 3 H, Ac), 2.87 (dd, 1 H, $J_{3\text{eq},3\text{ax}} = 12.8$, $J_{3\text{eq},4} = 4.6$, H-3eq), 3.60 (s, 3 H, Me), 4.00 (m, 1 H, H-6), 4.01 (q, 1 H, $J_{5,6} + J_{5,\text{NH}} = 29.0$, H-5), 4.08–4.10 (m, 1 H, H-9a), 4.32 (dd, 1 H, $J_{9\text{b},9\text{a}} = 11.7$, $J_{9\text{b},8} = 2.2$, H-9b), 4.88 (ddd, 1 H, $J_{4,5} = 14.2$, $J_{4,3\text{ax}} = 10.1$, H-4), 5.21 (d, 1 H, $J_{\text{NH},5} = 9.2$, NH), 5.26–5.30 (m, 2 H, H-7 + H-8), 7.63–7.65 (m, 2 H, Ar-H), 8.17–8.21 (m, 2 H, Ar-H). To a stirred solution of the peracetylated sialoside **5b**/glycal **6** mixture (875 mg) in methanol (15 mL) at room temperature was added a solution of sodium methoxide [5 mL, prepared from sodium metal (25 mg, 1.1 mmol) and methanol]. After 2 h, the reaction mixture was neutralized with Amberlite 120-(H $^+$) resin, filtered, and concentrated under reduced pressure to afford an off-white solid. Purification by silica gel chromatography using chloroform–methanol (8:1 to 5:1) as eluent afforded the methyl ester **7b** (288 mg, 32% over two steps) as a pale yellow solid: ^1H NMR (CD_3OD) δ 1.91 (dd, 1 H, $J_{3\text{ax},3\text{eq}} = 12.7$, $J_{3\text{ax},4} = 11.4$, H-3ax), 1.99 (s, 3 H, Ac), 2.88 (dd, 1 H, $J_{3\text{eq},4} = 4.7$, H-3eq), 3.44 (dd, 1 H, $J_{6,5} = 10.4$, $J_{6,7} = 1.6$, H-6), 3.47 (dd, 1 H, $J_{7,8} = 9.1$, H-7), 3.58–3.69 (m, 5 H, H-4 + H-9a + Me), 3.75 (ddd, 1 H,

¹ Abbreviations: CP, catalytic proficiency; DANA, 2-deoxy-2,3-didehydro-*N*-acetylneuraminic acid; NeuAc, *N*-acetylneuraminic acid; PFP-*S*-NeuAc, 2,3,4,5,6-pentafluorophenyl 2-thio- α -D-sialoside; PNP-*O*-NeuAc, *p*-nitrophenyl α -D-sialoside; PNP-*S*-NeuAc, *p*-nitrophenyl 2-thio- α -D-sialoside; MU-NeuAc, 4-methylumbelliferyl α -D-sialoside.

Scheme 1



$J_{8,9a} = 5.7$, $J_{8,9b} = 2.6$, H-8), 3.81 (dd, 1 H, $J_{9b,9a} = 11.4$, H-9b), 3.83 (t, 1 H, $J_{5,6} + J_{5,4} = 20.4$, H-5), 7.35–7.39 (m, 2 H, Ar-H), 7.83 (d, 1 H, $J = 8.9$, Ar-H), 8.23 (d, 1 H, Ar-H). A solution of the methyl ester **7b** (288 mg, 0.625 mmol) and lithium hydroxide monohydrate (112 mg, 2.67 mmol) in tetrahydrofuran–water (15 mL, 2:1) was stirred at 0 °C for 15 min and then at room temperature for 1.5 h. The reaction mixture was neutralized with Amberlite 120-(H+) resin, filtered, and concentrated under reduced pressure to afford the required 2-thiosialoside **2b** (253 mg, 91%). An analytical sample was prepared by silica gel chromatographic purification using ethyl acetate–methanol–water (20:2:1) as eluent to afford a yellow solid: R_f 0.16 (ethyl acetate–methanol–water, 10:2:1); mp 209 °C (dec); $[\alpha]_D^{20} = +89.0$ (c 0.417, ethanol); ^1H NMR (D_2O) δ 1.90 (t, 1 H, $J_{3ax,3eq} + J_{3ax,4} = 24.0$, H-3ax), 2.02 (s, 3 H, Ac), 2.91 (dd, 1 H, $J_{3eq,3ax} = 12.6$, $J_{3eq,4} = 4.8$, H-3eq), 3.53 (dd, 1 H, $J_{6,5} = 10.4$, $J_{6,7} = 1.9$, H-6), 3.56 (dd, 1 H, $J_{7,8} = 9.1$, H-7), 3.59 (dd, 1 H, $J_{9a,9b} = 11.9$, $J_{9a,8} = 6.0$, H-9a), 3.65–3.72 (m, 1 H, H-4), 3.75–3.78 (m, 1 H, H-8), 3.82 (dd, 1 H, $J_{9b,8} = 1.7$, H-9), 3.86 (t, 1 H, $J_{5,4} + J_{5,6} = 20.3$, H-5), 7.77 (d, 2 H, $J = 8.4$, Ar-H), 8.21 (d, 2 H, Ar-H); ^{13}C NMR (CD_3OD) δ 22.6 (Ac), 41.9 (C-3), 53.6 (C-5), 64.4 (C-9), 69.1 (C-7), 70.1 (C-4), 73.2 (C-8), 77.5 (C-6), 87.9 (C-2), 124.5 (Ar), 137.7 (Ar), 139.5 (Ar), 149.9 (Ar), 171.7 (Ac), 175.3 (C-1). Anal. Calcd for $\text{C}_{22}\text{H}_{28}\text{N}_2\text{O}_8\text{S}$: C, 45.74; H, 4.97; N, 6.27. Found: C, 45.36; H, 5.15; N, 5.97.

Measurement of Thiol pK_a Values. The pK_a values for 3,4-difluoro-, 4-bromo-, and 3,5-dimethylthiophenol were determined spectrophotometrically. Aliquots (50 μL) of the thiophenol (2×10^{-3} M in ethanol) were added to cuvettes containing ≥ 1 mL of KOAc–HOAc (50 mM, pH range ~ 4.0 – 5.5) or KH_2PO_4 – K_2HPO_4 (50 mM, pH range ~ 5.5 – 7.2) buffers of constant ionic strength ($I = 1.00$, KCl) at 25.0 ± 0.5 °C. UV/vis spectra (350–250 nm) were acquired immediately, and the pK_a values were calculated using a standard nonlinear least-squares fit (sigmoidal dose–response) of the absorbance versus pH data.

Enzyme Kinetics. Michaelis–Menten parameters for the wild-type, D92G mutant, and Y370G mutant enzymes were measured using analogous procedures to those reported earlier (11). Absorbance versus time data were recorded using an Olis Upgraded Cary 14 UV/vis spectrophotometer equipped with a circulating water bath temperature regulated six-cell block. Each 500 μL reaction was performed at 37.0 ± 0.5 °C by equilibrating the buffer (NaOAc–HOAc, pH 5.25, 100 mM) and substrate in the cell block for 3–5 min prior to the addition of enzyme (50 μL in 0.01% BSA). Kinetic parameters were determined from a minimum of seven initial rate measurements within a substrate concentration range of

at least $K_m/3$ to $4K_m$. Michaelis–Menten parameters were calculated using a standard nonlinear least-squares fit of the initial rate versus substrate concentration data.

Hydrolysis of **2a**, **2b**, and **2e** was monitored at 300 nm ($\Delta\epsilon = 1498 \text{ M}^{-1} \text{ cm}^{-1}$), 420 nm ($\Delta\epsilon = 8410 \text{ M}^{-1} \text{ cm}^{-1}$), and 283 nm ($\Delta\epsilon = 2543 \text{ M}^{-1} \text{ cm}^{-1}$), respectively. For **2a** and **2b**, reactions were performed in the presence of 2 mM 1,4-dithiothreitol. The wild-type-catalyzed reactions with **2c**, **2d**, and **2f–h** were performed in the presence of Ellman's reagent (2 mM), and the formation of 2-thio-5-nitrobenzoate was monitored at 412 nm ($\Delta\epsilon = 10900 \text{ M}^{-1} \text{ cm}^{-1}$) (32). The D92G and Y370G mutant-catalyzed hydrolyses of **2c** were monitored at 300 nm ($\Delta\epsilon = 2121 \text{ M}^{-1} \text{ cm}^{-1}$). Control experiments demonstrated that the rate of wild-type sialidase-catalyzed hydrolysis of MU-NeuAc was independent of the presence of DTT and that the corresponding rate of PNP-*O*-NeuAc hydrolysis was independent of the presence of Ellman's reagent. Estimations of k_{cat} for the hydrolyses of **2c–h** by D92G were determined by monitoring the sialic acid released at high substrate concentration (1 mM) (11).

Product Studies. ^1H NMR spectroscopy was employed to identify the products of the enzyme-catalyzed reactions (see Supporting Information). These reactions were conducted using a previously reported protocol (11).

RESULTS

Substrate Synthesis. The eight aryl 2-thio- α -D-sialosides were prepared from β -D-sialosyl chloride **4** (Scheme 1) (28, 31, 33, 34). During the coupling reaction some dehydrohalogenation of the *tert*-sialosyl chloride **4** occurred to generate the α,β -unsaturated ester **6** as an unwanted byproduct. This unsaturated ester could not be removed effectively from coupled products until the acetate protecting groups had been removed. The purified methyl ester was then saponified to give, after acidification and lyophilization, the desired aryl 2-thio- α -D-sialosides in yields of 87–100%. Flash chromatographic purification of the methyl esters (**7a–h**) and the aryl 2-thio- α -D-sialosides (**2a–h**) permitted the efficient removal of DANA. These crucial steps are important in order to ensure that the measurement of accurate kinetic data is not rendered impracticable by the presence of the tightly binding glycal impurity. Previously, this critical step had been accomplished using HPLC (35).

Enzyme Kinetics. Of note, the wild-type *M. viridifaciens* sialidase used in the present study was a newly purified pool of enzyme, and the measured kinetic parameters for this enzyme batch, assuming that the enzyme is 100% active, are about 2-fold greater than those estimated previously (11). Specifically, the newly measured values on the sialidase-

Table 1: Michaelis–Menten Kinetic Parameters for the Wild-Type Sialidase Measured at pH 5.25 and 37 °C^a

thiophenol substitution	pK _a ^b (log H ⁺)	k _{cat} (s ⁻¹)	k _{cat} /K _m (M ⁻¹ s ⁻¹)	K _m (mM)
pentafluoro (2a)	2.68 ^c	259 ± 8	(1.03 ± 0.14) × 10 ⁶	0.25 ± 0.03
4-nitro (2b)	4.50 ^c	196 ± 5	(6.67 ± 0.72) × 10 ⁵	0.29 ± 0.02
3,5-dichloro (2c)	4.94 ^d	66.3 ± 1.2	(1.04 ± 0.08) × 10 ⁵	0.64 ± 0.04
3,4-difluoro (2d)	5.63 ^e	9.43 ± 0.14	(4.7 ± 0.3) × 10 ³	2.02 ± 0.09
4-bromo (2e)	5.76 ^e	12.7 ± 1.0	(3.9 ± 1.1) × 10 ³	3.2 ₅ ± 0.7
4-chloro (2f)	5.97 ^d	6.60 ± 0.09	(3.99 ± 0.23) × 10 ³	1.65 ± 0.07
none (2g)	6.43 ^c	0.140 ± 0.003	(2.12 ± 0.27) × 10 ³	0.064 ± 0.007
3,5-dimethyl (2h)	6.58 ^e	4.49 ± 0.17	(1.42 ± 0.20) × 10 ³	3.17 ± 0.34

^a For wild-type-catalyzed hydrolysis of PNP-*O*-NeuAc, the *k*_{cat} and *k*_{cat}/*K*_m parameters are 277 ± 11 s⁻¹ and (1.7 ± 0.3) × 10⁷ M⁻¹ s⁻¹, respectively (11). ^b All p*K*_a values are at 25 °C (*I* = 1, KCl) in aqueous solution. ^c Reference 60. ^d Reference 61. ^e This study.

Table 2: Michaelis–Menten Kinetic Parameters for the D92G Mutant Sialidase Measured at pH 5.25 and 37 °C^a

thiophenol substitution	pK _a ^b (log H ⁺)	compd	k _{cat} (s ⁻¹)	k _{cat} /K _m (M ⁻¹ s ⁻¹)	K _m (μM)
pentafluoro	2.68 ^c	2a	13.6 ± 0.7	(4.8 ± 1.3) × 10 ⁶	2.8 ± 0.7
4-nitro	4.50 ^c	2b	11.2 ± 0.3	(5.4 ± 0.7) × 10 ⁶	2.1 ± 0.2
3,5-dichloro	4.94 ^d	2c	2.07 ± 0.21	ND ^e	ND ^e
3,4-difluoro	5.63 ^f	2d	0.53 ± 0.09	ND ^e	ND ^e
4-bromo	5.76 ^f	2e	0.85 ± 0.10	ND ^e	ND ^e
4-chloro	5.97 ^d	2f	0.89 ± 0.05	ND ^e	ND ^e
none	6.43 ^c	2g	0.26 ± 0.02	ND ^e	ND ^e
3,5-dimethyl	6.58 ^f	2h	0.11 ± 0.01	ND ^e	ND ^e

^a For wild-type-catalyzed hydrolysis of PNP-*O*-NeuAc, the *k*_{cat} and *k*_{cat}/*K*_m parameters are 18.6 ± 0.4 s⁻¹ and (5.6 ± 0.6) × 10⁶ M⁻¹ s⁻¹, respectively (18). ^b All p*K*_a values are at 25 °C (*I* = 1, KCl) in aqueous solution. ^c Reference 60. ^d Reference 61. ^e ND, not determined. ^f This study.

Table 3: Michaelis–Menten Kinetic Parameters for the Y370G Mutant Sialidase Measured at pH 5.25 and 37 °C^a

thiophenol substitution	pK _a ^b (log H ⁺)	compd	k _{cat} (s ⁻¹)	k _{cat} /K _m (M ⁻¹ s ⁻¹)	K _m (mM)
pentafluoro	2.68 ^c	2a	2.87 ± 0.14	2110 ± 410	1.4 ± 0.2
4-nitro	4.50 ^c	2b	0.321 ± 0.014	73 ± 11	4.4 ± 0.5
3,5-dichloro	4.94 ^d	2c	0.033 ± 0.003	25 ± 9	1.3 ± 0.3

^a For Y370G mutant-catalyzed hydrolysis of PNP-*O*-NeuAc, the *k*_{cat} and *k*_{cat}/*K*_m parameters are 123 ± 6 s⁻¹ and (1.1 ± 0.3) × 10⁶ M⁻¹ s⁻¹, respectively (15). ^b All p*K*_a values are at 25 °C (*I* = 1, KCl) in aqueous solution. ^c Reference 60. ^d Reference 61.

catalyzed hydrolysis of PNP-*O*-NeuAc for *k*_{cat} and *k*_{cat}/*K*_m are 277 ± 11 s⁻¹ and (1.7 ± 0.3) × 10⁷ M⁻¹ s⁻¹, respectively, while the previously reported values on *k*_{cat} and *k*_{cat}/*K*_m were 145 ± 7 s⁻¹ and (8.5 ± 1.7) × 10⁶ M⁻¹ s⁻¹, respectively (11). Presumably, the first pool of enzyme had a lower specific activity because the purification took longer as several steps required optimization. All subsequent purifications were performed more expediently, so the crude protein samples were not stored for any significant period of time.

During the initial screen for activity using the aryl 2-thiosialosides **2a–h**, it was observed that the first 5% of hydrolysis gave nonlinear absorbance versus time profiles. This observation presumably was a result of oxidation of the thiolate leaving groups, by dissolved oxygen, to the corresponding disulfides. Therefore, for the aryl 2-thiosialosides **2a** and **2b** the kinetic analyses were carried out in the presence of dithiothreitol (2 mM), a reducing agent which has been used to prevent thiol/thiolate oxidation (36), while for the aryl 2-thiosialosides **2c–h**, the kinetic data were acquired in the presence of Ellman's reagent (2 mM) (37). For the D92G mutant sialidase, Michaelis–Menten curves for the aryl 2-thiosialosides **2c–h** were not obtained because accurate kinetics could not be performed at low concentrations of substrate (~1–5 μM) due to the instability of these thiolate leaving groups under the reaction conditions. Therefore, only *k*_{cat} values were measured at high substrate concentrations by detecting the released sialic acid product.

Listed in Tables 1–3 are the kinetic parameters for the hydrolysis of the aryl 2-thio-α-D-sialosides with the *M. viridifaciens* recombinant wild-type, the D92G mutant, and the Y370G mutant sialidases. Shown in Figures 1 and 2 are the corresponding Brønsted plots. It is clear that the Brønsted plots for the wild-type and D92G mutant sialidases display nonlinear behavior. The derived β_{lg} values, for substrates with thiophenolate leaving groups of p*K*_a values ≥ 4.5, on *k*_{cat} and *k*_{cat}/*K*_m for the wild type are -0.83 ± 0.11 and -1.27 ± 0.17, respectively. The *k*_{cat} data point for the wild-type sialidase with **2g** was omitted from the β_{lg} calculation, while for the D92G mutant the β_{lg} value on *k*_{cat} for the same set of leaving groups is -0.82 ± 0.12. On the other hand, the Y370G mutant did not display a break in the Brønsted plots, and the derived β_{lg} values, for the three aryl 2-thiosialosides studied, on *k*_{cat} and *k*_{cat}/*K*_m are -0.76 ± 0.28 and -0.84 ± 0.04, respectively.

Product Studies. A product study of the wild-type-catalyzed hydrolysis of PNP-*S*-NeuAc (10 mM) in either the presence or absence of DTT (2 mM) clearly showed αNeuAc to be the first formed product, which subsequently underwent mutarotation to give βNeuAc (Figure S7, Supporting Information). No other sialoside product was detected in these experiments.

DISCUSSION

Compared to *O*-glycosides, the glycosidic linkage of exothioglycosides is more stable to both acid- (38) and

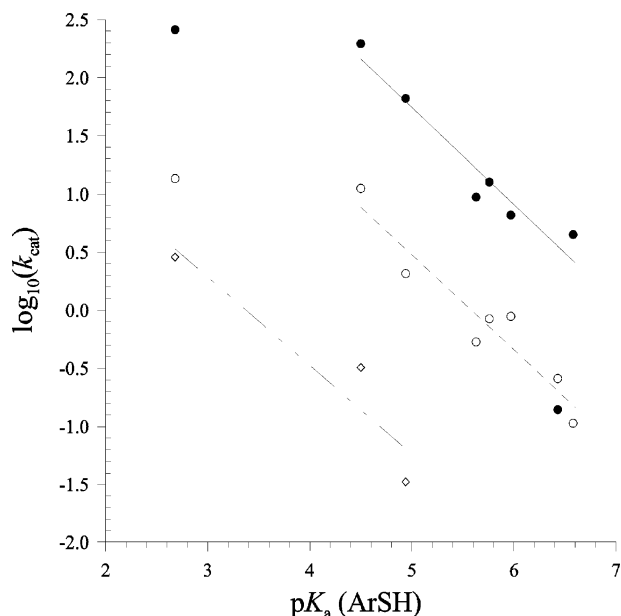


FIGURE 1: Brønsted plot. Effect of leaving group ability on k_{cat} for the wild-type sialidase (●) and D92G (○) and Y370G (◇) mutant sialidases. All experiments were performed at 37 °C and pH 5.25. The lines are the best linear fits to the data (see Results section for full details).

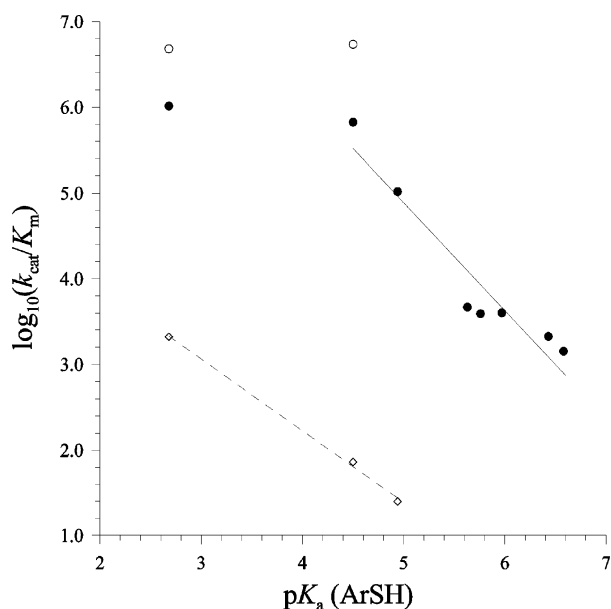


FIGURE 2: Brønsted plot. Effect of leaving group ability on $k_{\text{cat}}/K_{\text{m}}$ for the wild-type sialidase (●) and D92G (○) and Y370G (◇) mutant sialidases. All experiments were performed at 37 °C and pH 5.25. The lines are the best linear fits to the data (see Results section for full details).

enzyme-catalyzed hydrolysis (39). Consequently, thioglycosides have been developed for use: as glycosidase inhibitors (40), as substrate mimics for analysis of binding equilibria (41), as ligands for affinity chromatography (42), and as biological probes (43–45).

Nonetheless, thioglycosidase activity has been observed in nature in extracts of fungal (46), bacterial (47), and mammalian (48) species. Notably, the plant myrosinases (47, 49) and a human *O*-GlcNAcase (50) represent the only two examples of well-characterized thioglycoside-processing enzymes. Myrosinases are exothioglycosidases believed to be part of the plant defense system, and these enzymes differ

from other glycosidases in that they lack the strictly conserved catalytic acid residue (Glu) present in all other glycosidases from glycoside hydrolase family 1 (49). Their substrates, glucosinolates, possess an *O*-sulfated thiohydroxamic acid aglycon, and this good leaving group presumably does not require acid catalysis to depart. Recently, Vocadlo and co-workers reported that the human *O*-GlcNAcase (glycosidase family 84) catalyzes the efficient hydrolysis of aryl 2-acetamido-2-deoxy-1-thio- β -D-glucopyranosides (50). These authors postulated that this thioglycosidase activity might afford the cell protection from *S*-GlcNAc-modified proteins, which could result from aberrant glycosylation of cysteine residues, by *O*-GlcNAc transferase (OGTase) (50).

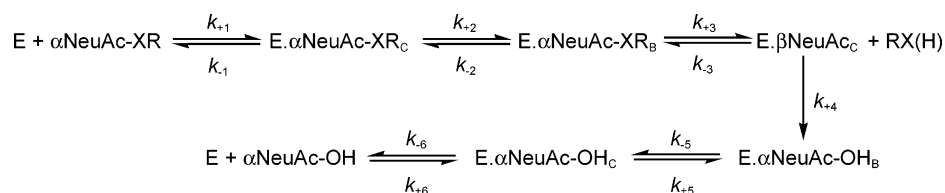
Within the realm of sialidases, various thiosialosides have been characterized as competitive inhibitors for various sialidases, including those from *Arthrobacter ureafaciens*, *Clostridium perfringens*, *V. cholerae*, influenza, rotavirus, and Newcastle disease virus (40, 44, 51–53). In addition, the sialidases from influenza and *V. cholerae* have been shown to have little or no hydrolytic activity against either thioglycoside analogues of natural (26, 53) or aryl-containing (51, 52) substrates. However, one recent report notes that the *T. rangeli* sialidase possesses thioglycosidase activity, cleaving thiosialoside **1** at approximately one-third of the rate of the natural oxygen homologue 2,3-sialyl lactose, although the precise values for the kinetic parameters (k_{cat} and $k_{\text{cat}}/K_{\text{m}}$) were not reported (54). Furthermore, these authors suggested that, on the basis of the observation that the glycal DANA was bound in the *T. rangeli* sialidase's active site after being soaked with **1**, the hydrolysis gave DANA as a side product. In addition, other researchers have attempted to use 2-thiosialosides as substrate mimics, to probe the structure of the Michaelis complex, for X-ray diffraction experiments on the *V. cholerae* and the influenza sialidases (9, 35). Interestingly, in none of these cases was any electron density observed that would be consistent with the thiosialoside being bound in the enzyme's active site. These observations suggest that the very slow turnover of the thiosialosides by these enzymes is certainly possible.

Mechanism of Sialidase-Catalyzed Thiosialoside Hydrolyses. The generally accepted mechanism for sialidase-catalyzed hydrolyses is shown in Scheme 2 (11, 55, 56). In this scheme, the first formed Michaelis complex undergoes a conformational change that results in a chair to boat transition of the substrate (k_{+2} , Scheme 2), which upon cleavage of the glycosidic bond (k_{+3}) forms an enzyme-bound intermediate that is covalently linked to the active site tyrosine residue (12, 14).

The product study for the wild-type sialidase-catalyzed reaction of PNP-*S*-NeuAc (**2b**) revealed that, like all other wild-type sialidases, hydrolysis proceeds with retention of anomeric configuration (Figure S7, Supporting Information). Significantly, the glycal DANA was not observed in the ^1H NMR spectra during the wild-type-catalyzed hydrolysis of **2b**, suggesting that the reaction of exothioglycosides, with this specific sialidase, follows a pathway similar to that of their oxygen counterparts (11, 15, 16).

The kinetic data for the sialidase-catalyzed hydrolysis of the aryl 2-thio- α -D-sialosides are consistent with the mechanism shown in Scheme 2 where, for the best leaving groups, k_2 is the rate-limiting step for the second-order rate constant ($k_{\text{cat}}/K_{\text{m}}$). That is, if deglycosylation (k_4) was rate limiting,

Scheme 2



then the wild-type enzyme should exhibit a larger second-order rate constant than the D92G mutant, a catalyst which should be incapable of general-base assistance during the deglycosylation step; i.e., k_{+4} (wild-type) $>$ k_{+4} (D92G). In addition, the leaving group has an effect on the magnitude of the second-order rate constant, for different leaving group chemistries, even though the respective Brønsted plots are flat. Specifically, for the wild-type-catalyzed hydrolysis of the most reactive oxygen- and sulfur-containing aglycons, the measured values for $k_{\text{cat}}/K_{\text{m}}$ are $(1.7 \pm 0.3) \times 10^7 \text{ M}^{-1} \text{ s}^{-1}$ (PNP-*O*-NeuAc) and $(1.03 \pm 0.14) \times 10^6 \text{ M}^{-1} \text{ s}^{-1}$ (PFP-*S*-NeuAc), respectively. In other words, glycosidic bond cleavage is not rate-determining, yet the leaving group is still present at the transition state for the first irreversible step, and this must be either k_{+1} or k_{+2} (Scheme 2). Specifically, if k_{+1} approaches the rate of diffusion, then the first irreversible step is the conformational change (k_{+2}); the $k_{\text{cat}}/K_{\text{m}}$ value for enzymes in which diffusion contributes to the rate-limiting step is typically around $10^8 \text{ M}^{-1} \text{ s}^{-1}$ (57).

With regard to the first-order rate constant (k_{cat}), the likely rate-determining step for the same activated leaving groups is deglycosylation for the following reasons: (i) the magnitude of the rate constant for the pentafluoro compound for the wild-type enzyme is identical to that for the hydrolysis of the oxygen-containing substrate PNP-*O*-NeuAc, (ii) the D92G mutant turns over activated substrates by a factor of approximately 20 less rapidly than does the wild-type enzyme, and (iii) the value of $\text{p}K_{\text{a}}$ (ArSH) has a negligible effect on the magnitude of k_{cat} . On the other hand, when the value for $\text{p}K_{\text{a}}$ (ArSH) is greater than 4.5, then the rate-limiting step for both the first- and the second-order rate constants involves C–S bond cleavage. Specifically, the β_{lg} values on k_{cat} and $k_{\text{cat}}/K_{\text{m}}$ for the wild-type-catalyzed hydrolysis are -0.83 ± 0.11 and -1.27 ± 0.17 , respectively. Under these circumstances the rate-determining step is identical for both kinetic constants; therefore, the difference between the two β_{lg} values necessitates that the thiolate is activated as a leaving group during formation of the Michaelis complex.

Given that both of the well-characterized thioglycosidases function without acid catalysis (49, 50), the kinetic parameters were measured for a general-acid mutant of the *M. viridifaciens* sialidase (D92G) (18). The derived β_{lg} value on k_{cat} for the D92G mutant sialidase-catalyzed hydrolysis of the less activated aryl 2-thiosialosides (-0.82 ± 0.12) is identical to that for the wild-type enzyme (-0.83 ± 0.11). As a result, it can be concluded that the wild-type and D92G mutant enzymes have similarly negligible degrees of protonation at their respective transition states for C–S bond cleavage. That is, both the wild-type and the general-acid/base mutant enzymes catalyze cleavage of the glycosidic C–S bond in thiosialosides, which are compounds where acid catalysis is effectively prohibited, by the correct alignment of a suitable nucleophile that is actively participating in the cleavage reaction ($\text{S}_{\text{N}}2$ -like).

This intrinsic property of thiols, that is, their inherent ineffectiveness in undergoing general-acid-catalyzed departure or general-acid-catalyzed nucleophilic substitution reactions at acetal centers, has been exploited by Withers and co-workers to make thioglycosidic linkages catalytically using mutant glycosidases with sulfur-containing carbohydrate acceptors (58, 59).

Conversely, the Y370G mutant enzyme is a very poor catalyst for the hydrolysis of aryl 2-thiosialosides (Table 3). This observation is consistent with the previous conclusions of Newstead et al., who argued that the Y370G mutant sialidase, in contrast to the wild-type enzyme, operates via a dissociative mechanism ($\text{S}_{\text{N}}1$ -like) in which a bound water molecule attacks the nascent oxacarbenium ion center following departure of the leaving group (15). In other words, there is little nucleophilic catalysis for the departure of bad leaving groups; in the present case the leaving groups are thiolate anions.

CONCLUSIONS

The sialidase from *M. viridifaciens* has been found to catalyze the hydrolysis of aryl 2-thio- α -D-sialosides with remarkable efficiency. The wild-type and D92G mutant enzymes exhibit a change in rate-determining step from glycosidic C–S bond cleavage for substrates in which the $\text{p}K_{\text{a}}$ of the conjugate acid of the leaving group is ≥ 4.5 , to either deglycosylation (k_{cat}) or a conformational change that occurs prior to C–S bond cleavage ($k_{\text{cat}}/K_{\text{m}}$) for the most activated leaving groups. In contrast, for the Y370G inverting sialidase, where water is the nucleophile, glycosidic C–S bond cleavage is rate-determining for both k_{cat} and $k_{\text{cat}}/K_{\text{m}}$. The enzyme-catalyzed hydrolysis of 2-thiosialosides is strongly catalyzed by the nucleophilic tyrosine residue but not by the general acid catalyst.

ACKNOWLEDGMENT

We thank the three anonymous reviewers for helpful comments.

SUPPORTING INFORMATION AVAILABLE

Experimental procedures for substrate synthesis, NMR data, and the enzymatic product study data. This material is available free of charge via the Internet at <http://pubs.acs.org>.

REFERENCES

- Saito, M., and Yu, R. K. (1995) Biochemistry and function of sialidases, in *Biology of the Sialic Acids* (Rosenberg, A., Ed.) pp 261–313, Plenum Press, New York.
- Henrissat, B. (1991) A classification of glycosyl hydrolases based on amino acid sequence similarities, *Biochem. J.* 280, 309–316.
- Henrissat, B., and Bairoch, A. (1993) New families in the classification of glycosyl hydrolases based on amino acid sequence similarities, *Biochem. J.* 293, 781–788.

4. Henrissat, B., and Bairoch, A. (1996) Updating the sequence-based classification of glycosyl hydrolases, *Biochem. J.* 316, 695–696.
5. Vimr, E. R. (1994) Microbial sialidases: Does bigger always mean better?, *Trends Microbiol.* 2, 271–277.
6. Koshland, D. E., Jr. (1953) Stereochemistry and the mechanism of enzymic reactions, *Biol. Rev.* 28, 416–436.
7. Friebolin, H., Keilich, G., Ziegler, D., and Supp, M. (1980) ^1H -NMR-spectroscopic evidence for the release of *N*-acetyl- α -D-neuraminic acid as the 1st product of neuraminidase action, *Biol. Chem. Hoppe-Seyler* 361, 697–702.
8. Chong, A. K. J., Pegg, M. S., Taylor, N. R., and von Itzstein, M. (1992) Evidence for a sialosyl cation transition-state complex in the reactivity of sialidase from influenza virus, *Eur. J. Biochem.* 207, 335–343.
9. Wilson, J. C., Angus, D. I., and von Itzstein, M. (1995) ^1H NMR evidence that *Salmonella typhimurium* sialidase hydrolyzes sialosides with overall retention of configuration, *J. Am. Chem. Soc.* 117, 4214–4217.
10. Davies, G., Sinnott, M. L., and Withers, S. G. (1998) Glycosyl transfer, in *Comprehensive Biological Catalysis* (Sinnott, M. L., Ed.) pp 119–209, Academic Press, San Diego.
11. Watson, J. N., Dookhun, V., Borgford, T. J., and Bennet, A. J. (2003) Mutagenesis of the conserved active-site tyrosine changes a retaining sialidase into an inverting sialidase, *Biochemistry* 42, 12682–12690.
12. Watts, A. G., Damager, I., Amaya, M. L., Buschiazio, A., Alzari, P., Frasch, A. C., and Withers, S. G. (2003) *Trypanosoma cruzi* trans-sialidase operates through a covalent sialyl-enzyme intermediate: Tyrosine is the catalytic nucleophile, *J. Am. Chem. Soc.* 125, 7532–7533.
13. Watts, A. G., and Withers, S. G. (2004) The synthesis of some mechanistic probes for sialic acid processing enzymes and the labeling of a sialidase from *Trypanosoma rangeli*, *Can. J. Chem.* 82, 1581–1588.
14. Watts, A. G., Oppezzo, P., Withers, S. G., Alzari, P. M., and Buschiazio, A. (2006) Structural and kinetic analysis of two covalent sialosyl-enzyme intermediates on *Trypanosoma rangeli* sialidase, *J. Biol. Chem.* 281, 4149–4155.
15. Newstead, S., Watson, J. N., Knoll, T. L., Bennet, A. J., and Taylor, G. (2005) Structure and mechanism of action of an inverting mutant sialidase, *Biochemistry* 44, 9117–9122.
16. Watson, J. N., Newstead, S., Narine, A., Taylor, G., and Bennet, A. J. (2005) Two nucleophilic mutants of the *Micromonospora viridifaciens* sialidase operate with retention of configuration via two different mechanisms, *ChemBioChem* 6, 1999–2004.
17. Varghese, J. N., and Colman, P. M. (1991) Three-dimensional structure of the neuraminidase of influenza virus A/Tokyo/3/67 at 2.2 Å resolution, *J. Mol. Biol.* 221, 473–486.
18. Watson, J. N., Newstead, S., Dookhun, V., Taylor, G., and Bennet, A. J. (2004) Contribution of the active site aspartic acid to catalysis in the bacterial neuraminidase from *Micromonospora viridifaciens*, *FEBS Lett.* 577, 265–269.
19. Sakurada, K., Ohta, T., and Hasegawa, M. (1992) Cloning, expression, and characterization of the *Micromonospora viridifaciens* neuraminidase gene in *Streptomyces lividans*, *J. Bacteriol.* 174, 6896–6903.
20. Albery, W. J., and Knowles, J. R. (1976) Evolution of enzyme function and development of catalytic efficiency, *Biochemistry* 15, 5631–5640.
21. Watson, J. N., Knoll, T. L., Chen, J. H., Chou, D. T. H., Borgford, T. J., and Bennet, A. J. (2005) Use of conformationally restricted pyridinium α -D-*N*-acetylneuraminides to probe specificity in bacterial and viral sialidases, *Biochem. Cell Biol.* 83, 115–122.
22. Gaskell, A., Crennell, S., and Taylor, G. (1995) The three domains of a bacterial sialidase: A β -propeller, an immunoglobulin module and a galactose-binding jellyroll, *Structure* 3, 1197–1205.
23. Newstead, S. L., Watson, J. N., Bennet, A. J., and Taylor, G. (2005) Galactose recognition by the carbohydrate-binding module of a bacterial sialidase, *Acta Crystallogr. D* 61, 1483–1491.
24. Sulzenbacher, G., Driguez, H., Henrissat, B., Schulein, M., and Davies, G. J. (1996) Structure of the *Fusarium oxysporum* endoglucanase I with a nonhydrolyzable substrate analogue: Substrate distortion gives rise to the preferred axial orientation for the leaving group, *Biochemistry* 35, 15280–15287.
25. Czjzek, M., Cicek, M., Zamboni, V., Burmeister, W. P., Bevan, D. R., Henrissat, B., and Esen, A. (2001) Crystal structure of a monocotyledon (maize ZMGLU1) β -glucosidase and a model of its complex with *p*-nitrophenyl β -D-thioglucoside, *Biochem. J.* 354, 37–46.
26. Wilson, J. C., Kiefel, M. J., Angus, D. I., and von Itzstein, M. (1999) Investigation of the stability of thiosialosides toward hydrolysis by sialidases using NMR spectroscopy, *Org. Lett.* 1, 443–446.
27. Eschenfelder, V., and Brossmer, R. (1987) Synthesis of *p*-nitrophenyl 5-acetamido-3,5-dideoxy- α -D-glycero-D-galacto-2-nonulopyranosidonic acid, a chromogenic substrate for sialidases, *Carbohydr. Res.* 162, 294–297.
28. Rothermel, J., and Faillard, H. (1990) Phase-transfer-catalyzed synthesis of aryl α -ketosides of *N*-acetylneuraminic acid. A 2-methylfluoran-6-yl glycoside of *N*-acetylneuraminic acid, 2-methyl-6-(5-acetamido-3,5-dideoxy- α -D-glycero-D-galacto-nonulopyranosylonic acid)xanthene-9-spiro-1'-isobenzofuran-3'-one, a new substrate for neuraminidase assay, *Carbohydr. Res.* 196, 29–40.
29. Sun, X. L., Kanie, Y., Guo, C. T., Kanie, O., Suzuki, Y., and Wong, C. H. (2000) Syntheses of C-3-modified sialylglycosides as selective inhibitors of influenza hemagglutinin and neuraminidase, *Eur. J. Org. Chem.*, 2643–2653.
30. Cao, S. D., Meunier, S. J., Andersson, F. O., Letellier, M., and Roy, R. (1994) Mild stereoselective syntheses of thioglycosides under PTC conditions and their use as active and latent glycosyl donors, *Tetrahedron: Asymmetry* 5, 2303–2312.
31. Zanini, D., and Roy, R. (1998) Practical synthesis of starburst PAMAM alpha-thiosialodendrimers for probing multivalent carbohydrate-lectin binding properties, *J. Org. Chem.* 63, 3486–3491.
32. Ellman, G. L., Courtney, K. D., Andres, V. J., and Featherstone, R. M. (1961) A new and rapid colorimetric determination of acetylcholinesterase activity, *Biochem. Pharmacol.* 7, 88–95.
33. Lee, T. S., Massova, I., Kuhn, B., and Kollman, P. A. (2000) QM and QM-E simulations on reactions of relevance to enzyme catalysis: trypsin, catechol *O*-methyltransferase, β -lactamase and pseudouridine synthase, *J. Chem. Soc., Perkin Trans. 2*, 409–415.
34. Roy, R., and Laferriere, C. A. (1990) Synthesis of protein conjugates and analogues of *N*-acetylneuraminic acid, *Can. J. Chem.* 68, 2045–2054.
35. Groves, D. R., Bradley, S. J., Rose, F. J., Kiefel, M. J., and von Itzstein, M. (1999) How pure is your thiosialoside? A reinvestigation into the HPLC purification of thioglycosides of *N*-acetylneuraminic acid, *Glycoconjugate J.* 16, 13–17.
36. Dalby, K. N., and Jencks, W. P. (1997) General acid catalysis of the reversible addition of thiolate anions to cyanamide, *J. Chem. Soc., Perkin Trans. 2*, 1555–1563.
37. Zhou, Y., Guo, X. C., Yi, T., Yoshimoto, T., and Pei, D. H. (2000) Two continuous spectrophotometric assays for methionine aminopeptidase, *Anal. Biochem.* 280, 159–165.
38. Capon, B. (1969) Mechanism in carbohydrate chemistry, *Chem. Rev.* 69, 407–498.
39. Driguez, H. (2001) Thioligosaccharides as tools for structural biology, *ChemBioChem* 2, 311–318.
40. Kiefel, M. J., Beisner, B., Bennett, S., Holmes, I. D., and von Itzstein, M. (1996) Synthesis and biological evaluation of *N*-acetylneuraminic acid-based rotavirus inhibitors, *J. Med. Chem.* 39, 1314–1320.
41. Barr, B. K., and Holeywinski, R. J. (2002) 4-methyl-7-thioumbelliferyl- β -D-cellobioside: A fluorescent, nonhydrolyzable substrate analogue for cellulases, *Biochemistry* 41, 4447–4452.
42. Piyachomkwan, K., and Penner, M. H. (1998) Aryl thioglycoside-based affinity purification of exo-acting cellulases, *Anal. Biochem.* 255, 223–235.
43. Rich, J. R., and Bundle, D. R. (2004) S-linked ganglioside analogues for use in conjugate vaccines, *Org. Lett.* 6, 897–900.
44. Sabesan, S., Neira, S., Davidson, F., Duus, J. O., and Bock, K. (1994) Synthesis and enzymatic and NMR-studies of novel sialoside probes: Unprecedented, selective neuraminidase hydrolysis of and inhibition by C-6-(methyl)-Gal sialosides, *J. Am. Chem. Soc.* 116, 1616–1634.
45. Park, S., Lee, M. R., Pyo, S. J., and Shin, I. (2004) Carbohydrate chips for studying high-throughput carbohydrate-protein interactions, *J. Am. Chem. Soc.* 126, 4812–4819.
46. Reese, E. T., Clapp, R. C., and Mandels, M. (1958) A thioglucosidase in fungi, *Arch. Biochem. Biophys.* 75, 228–242.
47. Meulenbeld, G. H., and Hartmans, S. (2001) Thioglucosidase activity from *Sphingobacterium* sp strain OTG1, *Appl. Biochem. Biotechnol.* 56, 700–706.
48. Goodman, I., Fouts, J. R., Bresnick, E., Menegas, R., and Hitchings, G. H. (1959) Mammalian thioglycosidase, *Science* 130, 450–451.

49. Burmeister, W. P., Cottaz, S., Driguez, H., Iori, R., Palmieri, S., and Henrissat, B. (1997) The crystal structures of *Sinapis alba* myrosinase and a covalent glycosyl-enzyme intermediate provide insights into the substrate recognition and active-site machinery of an *S*-glycosidase, *Structure* 5, 663–675.
50. Macauley, M. S., Stubbs, K. A., and Vocadlo, D. J. (2005) *O*-GlcNAcase catalyzes cleavage of thioglycosides without general acid catalysis, *J. Am. Chem. Soc.* 127, 17202–17203.
51. Privalova, I. M., and Khorlin, A. Y. (1969) Substrates and inhibitors of neuraminidase. I. Synthesis of *O*-, *S*-, and *N*-ketosides of *N*-acetyl-D-neuraminic acid, *Izv. Akad. Nauk SSSR* 12, 2785–2792.
52. Khorlin, A. Y., Privalova, I. M., Zakstelskaya, L. Y., Molibog, E. V., and Evstigneeva, N. A. (1970) Synthetic inhibitors of *Vibrio cholerae* neuraminidase and neuraminidases of some influenza virus strains, *FEBS Lett.* 8, 17–19.
53. Suzuki, Y., Sato, K., Kiso, M., and Hasegawa, A. (1990) New ganglioside analogues that inhibit influenza-virus sialidase, *Glycoconjugate J.* 7, 349–356.
54. Amaya, M. F., Buschiazzi, A., Nguyen, T., and Alzari, P. M. (2003) The high-resolution structures of free and inhibitor-bound *Trypanosoma rangeli* sialidase and its comparison with *T. cruzi* trans-sialidase, *J. Mol. Biol.* 325, 773–784.
55. Guo, X., Laver, W. G., Vimr, E., and Sinnott, M. L. (1994) Catalysis by two sialidases with the same protein fold but different stereochemical courses: A mechanistic comparison of the enzymes from influenza A virus and *Salmonella typhimurium*, *J. Am. Chem. Soc.* 116, 5572–5578.
56. Chou, D. T. H., Watson, J. N., Scholte, A. A., Borgford, T. J., and Bennet, A. J. (2000) Effect of neutral pyridine leaving groups on the mechanisms of influenza type A viral sialidase-catalyzed and the spontaneous hydrolysis reactions of α -D-*N*-acetylneuraminides, *J. Am. Chem. Soc.* 122, 8357–8364.
57. Fersht, A. (1985) *Enzyme Structure and Mechanism*, 2nd ed., pp 147–154, W. H. Freeman, New York.
58. Jahn, M., Marles, J., Warren, R. A. J., and Withers, S. G. (2003) Thioglycoligases: Mutant glycosidases for thioglycoside synthesis, *Angew. Chem., Int. Ed. Engl.* 42, 352–354.
59. Jahn, M., Chen, H. M., Mullegger, J., Marles, J., Warren, R. A. J., and Withers, S. G. (2004) Thioglycosynthases: double mutant glycosidases that serve as scaffolds for thioglycoside synthesis, *Chem. Commun.*, 274–275.
60. Jencks, W. P., and Salvesen, K. (1971) Equilibrium deuterium isotope effects on ionization of thiol acids, *J. Am. Chem. Soc.* 93, 4433–4436.
61. Wilson, J. M., Bayer, R. J., and Hupe, D. J. (1977) Structure-reactivity correlations for thiol-disulfide interchange reaction, *J. Am. Chem. Soc.* 99, 7922–7926.

BI0607507